

Finite element analyses of the interaction of a pair of shield tunnels

Élément d'analyse finie de l'interaction d'une paire de tunnels réalisés par le creusement en bouclier

H. Akagi – Waseda University, Tokyo, Japan
K. Komiya – Chiba Institute of Technology, Japan

ABSTRACT: This paper introduces a numerical simulation procedure for use with the shield tunnelling problems and compares the simulation results with field measurements for soft clay ground. The shield machine advance is simulated numerically by adopting excavation elements and repetitively rearranging the three-dimensional finite element mesh used in the simulation. Deformation of soft clay ground and the effective stress behaviour as the shield machine advances under actual hydraulic jacking forces are modelled successfully by the new procedure. As an example, the application of this procedure to the twin shield tunnelling problem is described.

RESUME: Ce papier introduit une simulation numérique pour le problème du tunnel de rempart et compare les résultats de simulation avec le mesurage du champ des constructions. L'avance pour la machine rempart est simulée numériquement en adoptant des éléments d'excavation et en réarrangeant de façon répétitive la maille tridimensionnelle utilisée dans la simulation. Le nouveau procédé calcule une déformation des argiles terre et la conduite des pressions efficaces pendant que la machine rempart avance sous l'effet de forces hydrauliques qui sont modélisés, avec succès, par la nouvelle méthode. Pour donner un exemple, l'application de cette méthode au problème d'une paire de tunnels de rempart est décrite.

1 INTRODUCTION

Over the last three decades, shield tunnelling has become one of the most important procedures used in the construction of urban tunnel structures. In urban areas, it is essential to protect pre-existing structures and underground conduits from damage during shield tunnelling. To accomplish this, it is necessary to predict the influence of tunnelling on neighbouring structures. Predictions of ground stress and deformation behaviour during shield tunnelling have recently been carried out by numerical analysis based on the finite element method.

Further, where a pair of shield tunnels are constructed, a second tunnel is often excavated in parallel with the pre-existing first tunnel. The clearance between parallel tunnels has been reduced below $0.5 \cdot D$ (D : Diameter of tunnel). Under this situation, it is essential to evaluate the earth pressure acting on the tunnels for better prediction.

However, the finite element method generally used in shield tunnel design practice has been found to be too simple to model the actual processes of shield tunnelling. In particular, there have been many problems with finite element simulations of continuous excavation at the cutting face and of the tunnelling machine advancement processes.

This paper describes a new finite element technique, which takes the construction processes of shield tunnelling into account. The numerical analysis results using this technique are first demonstrated to show the effectiveness of the technique. Finally, simulation of the constructing twin shield tunnels is presented to show the changes in earth pressure acting on the tunnels at the time of construction.

2 SOIL-WATER COUPLED FINITE ELEMENT MODELLING OF SHIELD TUNNELLING

Shield tunnelling causes extreme disturbances in the soil adjacent to the cutting head during excavation. Excavation elements are defined in front of the cutting head as a proposed method of representing the area of ground being disturbed by the excavation.

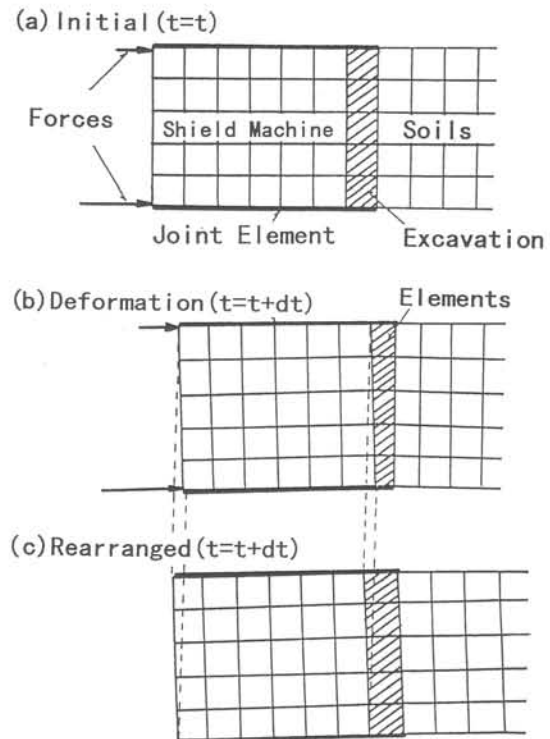


Figure 1. Advancement of the shield machine simulated by the excavation elements.

Figure 1 depicts the sequential behaviour of the finite element model as excavation is carried out by the cutting head and the tunnelling machine advances. The shaded elements in Fig.1 represent the excavation elements. Since these are

greatly disturbed, their rigidity is small. Jacking forces act on the nodal points at the tail ends of shield machine at reference time t in Fig.1(a). The values of these forces were obtained from field measurements of hydraulic jack pressure. The excavation elements and other elements within the ground adjacent to the shield machine deform simultaneously under undrained or partly drained conditions due to these forces during time period dt , as shown in Fig.1(b). Since the rigidity of elements within the shield machine itself is much greater than those of other elements, deformation of the shield machine elements can be neglected.

After computing the displacements and stresses in the mesh arrangement shown in Fig.1(b), the finite element meshes are then rearranged as shown in Fig.1(c) with the correct stress and displacement fields to bring the geometric shape and size of the excavation element back to the original shown in Fig.1(a).

By repeating the procedure followed in Fig.1, the advancement of a shield machine and the associated changes in the stress-strain fields can be reproduced numerically using the finite element method.

Excavation and advancement cause large-magnitude deformations of the excavation elements in the direction of the force. Mesh rearrangement is necessary to avoid excessive deformation of the mesh. It is possible to introduce into the calculation, factors to account for the various practical execution procedures such as the clay slurry and water pressure acting on the cutting face in a slurry-type shield machine.

To simulate the pore water and soil interaction in the saturated ground, it is necessary to introduce into the analysis the coupling between deformation of the soil skeleton and movement of pore water. The finite element method can be used to incorporate this into the stress-deformation analysis of the saturated soil-water system. The effective stress change in a finite element is obtained from the displacement vector at the nodal points constituting that element. When the model is rearranged, a correct effective stress field can be obtained from the displacement vector of the rearranged nodal points. The method used to obtain correct values of effective stress and pore water pressure in the rearranged finite element mesh within the ground is described in the recent publication (Akagi and Komiya, 1996).

3 THREE-DIMENSIONAL ELASTO-PLASTIC FINITE ELEMENT SIMULATION OF SHIELD TUNNELLING

During shield tunnelling, the position and movement of the shield machine is controlled by means of hydraulic jacks fitted behind it. Consequently, the orientation and direction of movement of the shield machine can vary in three directions; that is, the pitching and yawing motion of the shield machine can be complicated. Moreover, complex boundary conditions exist, particularly when shield tunnelling in urban areas, since the clearance between the tunnel and pre-existing underground structures is frequently very small. Accordingly, the three-dimensional effects of shield tunnelling on the neighbouring environment must be considered if rational design of shield tunnelling is to be achieved.

In this section, a three-dimensional finite element analysis was carried out, taking account of the excavation procedures used in practical shield tunnel work and making use of the method described in the previous section. A practical example is adopted here: shield tunnelling with balanced earth pressure in the deep alluvial clay deposits found in the suburbs of Tokyo. The overburden depth is 32.8 m.

3.1 Outline of analysis

An ideal elastic constitutive equation, Hooke's law, was used for both shield machine elements and excavation elements. An elasto-plastic constitutive equation, the inviscid Sekiguchi-Ohta model, was used for the clay (Ohta and Sekiguchi, 1979). Shield machine propulsion was numerically simulated by applying forces

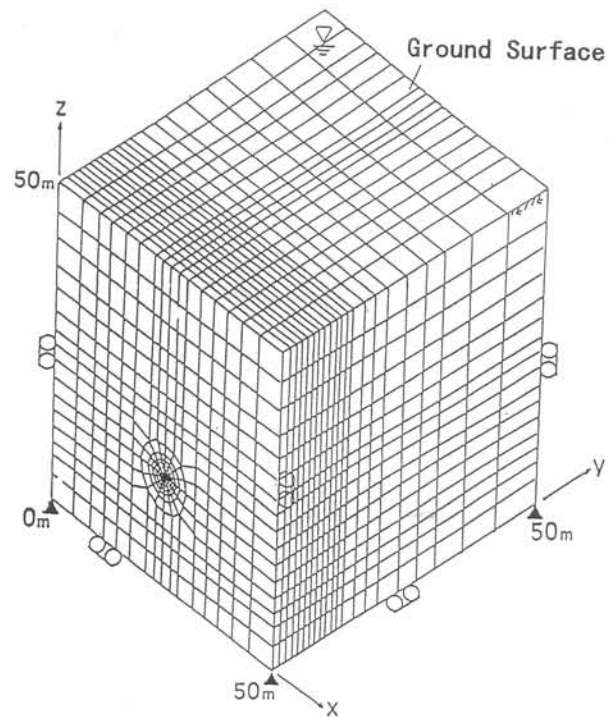


Figure 2. Finite element model used in the shield tunnelling simulation.

to the tail of the machine of a magnitude actually used to drive a shield machine. The three-dimensional finite element mesh is shown in Fig.2. The finite elements are the eight-noded isoparametric elements. The diameter of the shield machine is 3.737m and its length is 5.67m. The initial y-coordinate of the tail of the machine was arranged to be 2m in Fig.2 and the shield machine was driven forward in the positive y-axis direction. Excavation elements were placed in front of the shield machine; they had a thickness of 20 cm. The air bubble pressure used in the actual construction was applied within the excavation elements.

The input material parameters for clay were obtained on the basis of the standard geotechnical tests on undisturbed samples at various depths. The value of the compression index, λ , for the clay was 0.320, the swelling index, κ , was 0.054, and the critical state parameter, M , was 1.05. The range of the initial void ratio, e_0 , for the clay was from 1.65 to 1.73 dependent on the depth. Any needed parameters which could not be obtained from these tests were calculated using the method suggested by Izuka (1988).

Since the excavation elements represent the volume disturbed by cutting and slurry mixing in front of the cutting face, the material properties of the excavation elements were difficult to obtain from experimental procedures. The excavation elements were assumed to be elastic with an elastic modulus as determined below. In this analysis, the excavated volume of soil, i.e., the amount by which the machine advances at each jacking, is governed by the volume change and shear distortion of the excavation elements. Thus, the elastic modulus of the excavation elements was extremely important. A preliminary analysis was carried out by trial and error numerical simulations of excavation. An elastic modulus for each excavation element was obtained such that the shield advancement was equal to that in the field. The value of Young's modulus obtained in this preliminary analysis was 138.3(kN/m²) and the Poisson's ratio ν of the excavation elements was equal to 0.100.

3.2 Stress-deformation analysis of soft clay during shield tunnelling

In this section, the finite element simulation results of the stress-deformation behaviour of the soft clay during shield tunnelling are demonstrated.

Figures 3(a) and (b) indicate the deformation behaviour of soft clay due to the occurrence of tail void behind the shield machine obtained at the points in the ground initially 1 m above the crown of the shield machine. The three-dimensional view of the settlement trough within the ground is shown in Fig.3(a). The geometrical shape of the trough is similar to the field observation (Peck, 1969). Figure 3(b) depicts a horizontal view of the distribution of the vertical displacement obtained at the same situation as above. Vertical settlement due to the occurrence of tail void behind the tail of the shield machine amounts to 6 mm and this value is almost the same as the field measurement. The upheaval of the soft clay in front of the shield machine face is obtained due to the advancement of the machine in the y-direction. Since the machine is driven in the left direction, the upheaval of soft clay is extended in the same direction.

The effective stress paths in the soft clay around the shield machine during its advancement are shown in Fig.4. Eight elements in the vicinity of the circumferential face of shield machine are selected and the variations of mean effective stress p' and $\sqrt{2}J_2$ of each element are plotted throughout the machine advancement. The initial K_0 line, the critical state line and the current yield surface are also plotted in the figures. The elements designated by solid circles around the crown of shield machine are unloaded by the stress release during the shield advancement and the effective stress states move within the current yield surfaces. The elements designated by open circles below the invert of the machine are loaded by the weight of the machine and the jack operation. Most of their current yield surfaces are enlarged from their initial yield surfaces.

4 APPLICATION TO TWIN SHIELD TUNNELLING

In this section, the new procedure was applied to the twin shield tunnelling problems. The input parameters for ground conditions and the input data for the loads acting on the tail of the shield machine were the same as in the previous calculation. A pre-existing first tunnel of the same diameter ($D=3.737\text{m}$) as the second tunnel was assumed to be located at a distance of $0.5D$.

Figure 5 shows the time-dependent variation in earth pressure change ratio ($=(\text{pressure change})/(\text{initial pressure})$) acting on the first tunnel obtained at its springline and at the crown. Figure 6 gives the field measured earth pressure variations during the excavation of the second shield tunnel under similar soil and geometrical boundary conditions (Horichi et al., 1990). A remarkable increase in earth pressure at the springline was observed in the field, and similar calculation results are obtained in Fig.5. A gradual decrease in earth pressure at the crown was measured and this is similar to the numerical calculation results shown in Fig.5. Table 1 compares the values of earth pressure obtained from field measurement records with the numerical simulation results. Since the overburden in the calculation case is much greater than that in the field, the absolute values of earth pressure in the finite element calculation are different. However, as a ratio, the values of earth pressure change (R and R') are almost the same as the field measurements.

5 CONCLUSIONS

This paper introduces a new finite element technique to simulate construction processes of shield tunnelling. Excavation elements are proposed for the area in front of the cutting face. These represent the soil disturbed by cutting. A repetitive rearrangement of the finite element mesh is used in the calculation. A stress-deformation analysis of clay ground during shield tun-

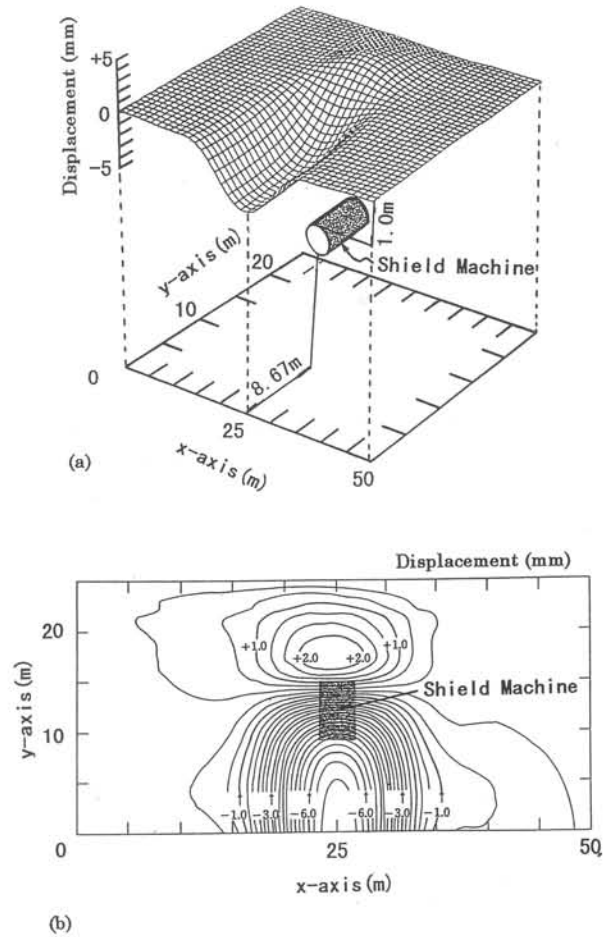


Figure 3. Deformation behaviour of soft clay due to the occurrence of a tail void.

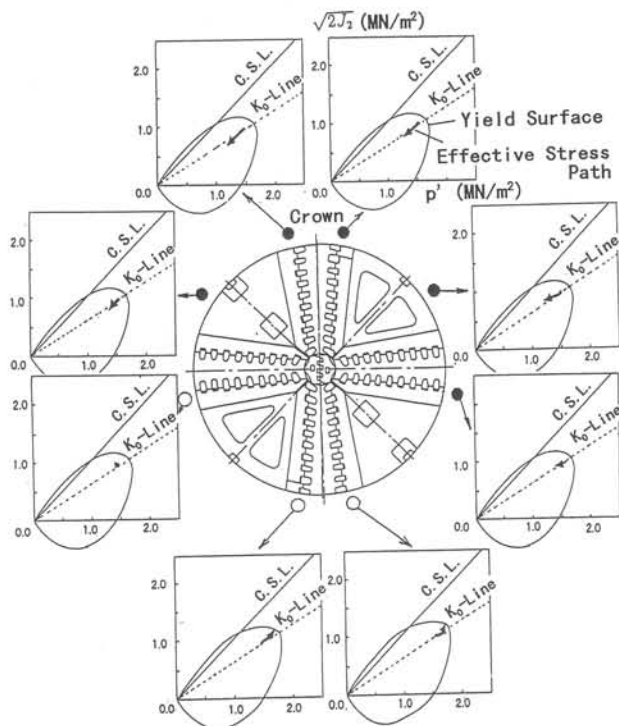


Figure 4. Effective stress paths of soft clay during shield machine advancement.

Table 1. Comparison of earth pressure changes during twin shield tunnelling.

Legend	Measured at 1	Calculated at 1	Measured at 2	Calculated at 2
Initial Value p_0 (kN/m ²)	220	520	180	490
Face Arrival p_1 (kN/m ²)	300	675	165	520
Ratio $R = (p_1 - p_0)/p_0$	0.36	0.30	-0.08	0.06
Tail Passing p_2 (kN/m ²)	205	484	150	435
Ratio $R' = (p_2 - p_0)/p_0$	-0.07	-0.07	-0.17	-0.11

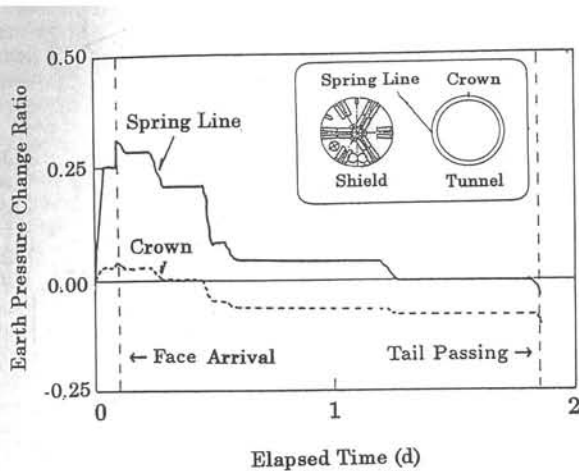


Figure 5. Time dependent variation in earth pressure.

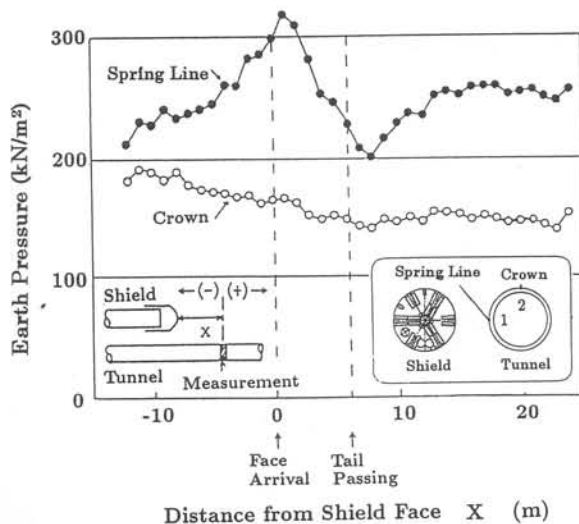


Figure 6. Field earth pressure variations.

nelling was carried out using this finite element method, taking into account the actual construction process. The results were compared with field measurements. An example demonstrating the application of the proposed procedure to the twin shield tunnelling problem was shown. From a comparison between the finite element calculation results and field measurements, it can be concluded that:

- (1) Advancement of the shield machine can successfully be simulated using the excavation elements and the repetitive mesh rearrangement proposed here.
- (2) Three-dimensional finite element simulation results for vertical ground displacement profile and effective stress paths of soft clay are obtained and coincide with the field observations.
- (3) The changing earth pressure acting on the pre-existing

tunnel during shield machine advance is successfully simulated by the proposed finite element simulation procedure.

ACKNOWLEDGEMENTS

The authors would like to express the gratitude to Tokyo Electric Power Company, who provided the field measurement records used in this study. Thanks are also due to Dr. Malcolm Bolton of Cambridge University, who suggested the three-dimensional representation of settlement trough using the finite element simulation results.

REFERENCES

- Akagi, H. and K. Komiya 1996. Finite element simulation of shield tunnelling processes in soft ground. *Proc. International Symposium of Technical Committee TC28 : Underground Construction in Soft Ground, 1996 (in print)*.
- Horichi, N. et al. 1990. Evaluation of axial rigidity of shield tunnel considering the shear characteristics of interface materials. *Proc. JSCE*, No.415, 251-259 (in Japanese).
- Iizuka, A. 1988. Study on the deformation and stability analyses of soft ground. Ph.D. Thesis, Kyoto University, 57-67 (in Japanese).
- Ohta, H. and H. Sekiguchi 1979. Constitutive equations considering anisotropy and stress reorientation in clay. *Proc. 3rd ICNMG*, 475-484.
- Peck, R.B. 1969. Deep excavations and tunnelling in soft ground. *State of the Art Report, 7th ICSMFE*, 225-290.